Sustainable Civil Infrastructures

Hany Shehata
Sherif El-Badawy *Editors*

Sustainable Issues in Infrastructure Engineering

The official 2020 publication of the Soil-Structure Interaction Group in Egypt (SSIGE)

Springer

Sustainable Civil Infrastructures

Sustainable Civil Infrastructures (SUCI) is a series of peer-reviewed books and proceedings based on the best studies on emerging research from all fields related to sustainable infrastructures and aiming at improving our well-being and day-to-day lives. The infrastructures we are building today will shape our lives tomorrow. The complex and diverse nature of the impacts due to weather extremes on transportation and civil infrastructures can be seen in our roadways, bridges, and buildings. Extreme summer temperatures, droughts, flash floods, and rising numbers of freeze-thaw cycles pose challenges for civil infrastructure and can endanger public safety. We constantly hear how civil infrastructures need constant attention, preservation, and upgrading. Such improvements and developments would obviously benefit from our desired book series that provide sustainable engineering materials and designs. The economic impact is huge and much research has been conducted worldwide. The future holds many opportunities, not only for researchers in a given country, but also for the worldwide field engineers who apply and implement these technologies. We believe that no approach can succeed if it does not unite the efforts of various engineering disciplines from all over the world under one umbrella to offer a beacon of modern solutions to the global infrastructure. Experts from the various engineering disciplines around the globe will participate in this series, including: Geotechnical, Geological, Geoscience, Petroleum, Structural, Transportation, Bridge, Infrastructure, Energy, Architectural, Chemical and Materials, and other related Engineering disciplines.

SUCI series is now indexed in SCOPUS
and EI Compendex.

More information about this series at http://www.springer.com/series/15140

Hany Shehata · Sherif El-Badawy
Editors

Sustainable Issues in Infrastructure Engineering

The official 2020 publication of the Soil-Structure Interaction Group in Egypt (SSIGE)

Springer

Editors
Hany Shehata
CEO of SSIGE
Cairo, Egypt

Sherif El-Badawy
Mansoura University
Mansoura, Egypt

ISSN 2366-3405 ISSN 2366-3413 (electronic)
Sustainable Civil Infrastructures
ISBN 978-3-030-62585-6 ISBN 978-3-030-62586-3 (eBook)
https://doi.org/10.1007/978-3-030-62586-3

This Springer imprint is published by the registered company Springer Nature Switzerland AG
The registered company address is: Gewerbestrasse 11, 6330 Cham, Switzerland

Contents

SSIGE Official Publications 2020: Part 2

FE Modeling of RC Beams Reinforced in Flexure with BFRP Bars Exposed to Harsh Conditions

Hakem Alkhraisha, Haya Mhanna, and Farid Abed(✉)

Civil Engineering, American University of Sharjah, Sharjah, UAE
fabed@aus.edu

Abstract. This paper aim to investigate the effect harsh conditions have on the flexural behavior of concrete beams reinforced longitudinally with Basalt Fiber Reinforced Polymer (BFRP) bars. Finite element (FE) software, ABAQUS, is used to develop a nonlinear model capable of simulating the behavior of exposed FRP reinforced beams in flexure. Data extracted from the numerical simulations were compared with experimental data to validate the FE model. Through a parametric study, this paper aims to study the effect of reducing the modulus of elasticity on BFRP reinforced beams. The values of modulus of elasticity are reduced from the by 10%, 20%, and 30% and the impact is observed. The paper also presents comparative analysis among different BFRP tensile strength values. The analysis of the effect of varying tensile strength values on the behavior of BFRP RC beams will be conducted on an under-reinforced beam. The BFRP tensile strength value is reduced by 10%, 20%, and 30% and the impact is observed. The results show that the reduction of the modulus of elasticity of the BFRP bar decreased the flexural capacity of the BFRP RC beam proportionally. The proportional decrease was not affected by the number of reinforcement bars used in the beams with similar axial stiffness. In addition, a reduction the tensile strength of the BFRP bars caused a disproportional decrease in the flexural capacity of the beams. Beams with lower tensile strength values failed at lower deflections.

1 Introduction

Fiber Reinforced Polymer (FRP) reinforcement was created to combat as an alternative to the conventional steel reinforcements. FRP products are non-metallic material which makes then non-corrosive (ACI 440 2015). Furthermore, FRP composites possess larger tensile strength than steel (ACI 440 2015; Bedard 1992). FRP reinforcements have different chemical composition and exhibit different failure modes than steel reinforcements do. Therefore, the conventional design philosophies of reinforced concrete had to be altered to account for the different mechanical behavior of FRP reinforcement. FRP reinforcement does not have unified material properties. Their properties depend on fiber type, fiber volume, fiber orientation, resin type, and quality control during the development process (ACI 440 2015). Despite the discrepancies in properties, all types of FRP bars are made of high strength fibers such as basalt, carbon, glass or aramid, combined together by a polymer resin (ACI 440 2015; Bedard 1992).

FRP bars are anisotropic materials that show linear elastic behavior until rupture (440 2015; Bedard 1992). Furthermore, FRP bars have lower modulus of elasticity than

H. Shehata and S. El-Badawy (Eds.): *Sustainable Issues in Infrastructure Engineering*, SUCI, pp. 3–13, 2021.
https://doi.org/10.1007/978-3-030-62586-3_1

steel (440 2015; El Messalami et al. 2019 Bedard 1992; Hollaway 2003). The ultimate tensile strength of FRP bars is indirectly related to their size; in other words an increase in diameter decreases the tensile strength (Hollaway 2003).

BFRP reinforcement, being a more recent development, has fewer studies about its flexural and shear behaviors (Abed and Alhafiz 2019; Abed et al. 2019; El Refai and Abed 2016; Elgabbas et al. 2017; El Refai et al. 2015; Fam and Tomlinson 2015; Abed et al. 2012). Elgabbas et al. studied the behavior of over-reinforced beams under static loads. The results showed that the increase in reinforcement ratio caused a non-linear increase in the flexural capacity of the beams (Elgabbas et al. 2017). Tomlinson et al. studied the performance of beams reinforced with BFRP in flexure and shear. Nine beams with reinforcement ratio ranging from 0.28 to 1.60 were casted. The results showed that the ultimate and service loads were proportionally impacted by the reinforcement ratio. The mode of failure of the nine beams depended on the reinforcement ratio and shear reinforcement (Fam and Tomlinson 2015).

Some researchers investigated the effect of exposure on the bond behavior between BFRP bars and concrete and on the flexural behavior of BFRP RC beams. The studies varied from examining the mechanical behavior of exposed FRP bars to investigating the effects of exposure on BFRP RC beams. Furthermore, studies had investigated the effects of Alkaline solutions (Al Rifai et al. 2020; Sim et al. 2005; Wang et al. 2008; Wu et al. 2015), temperature (El Refai et al. 2014; Calvet et al. 2015; D'Antino et al. 2018; Masmoudi et al. 2011; Robert et al. 2009), and saline solutions (Altalmas et al. 2015; Yan and Lin 2017; Al-Tamimi et al. 2014).

Wu et al. studied tensile properties of BFRP bars exposed to alkaline solution, salt solution, acid solution, and deionized water (Wu et al. 2015). The study utilized scanning electronic microscopy (SEM) to monitor the degradation mechanism of BFRP bars in an alkaline environment. The results indicated that acid, salt, and deionized water had a lower impact on the durability of BFRP bars than the alkaline solution did (Wu et al. 2015). Sim et al. examined the durability of basalt, glass, and carbon fiber exposed to alkali solution combined with high temperatures (Sim et al. 2005). The results showed that after seven days exposure, basalt and glass FRPs lost 50% of their strength and volume. Carbon FRP, however, only lost 13% of its strength during the same exposure time. The resin and fiber type played a big role in degradation resistance and since GFRP and BFRP had almost the same chemical composition they degraded at similar rate. The CFRP, however, did not face any relatively significant degradation. Wang et al. had also studied the durability of BFRP exposed to alkali solution (Wang et al. 2008). After three months of exposure the strength decrease by 40% but the modulus of elasticity remained unaffected. The results also indicated BFRP had lower degradation than the basalt fiber with no resin protection (Wang et al. 2008).

Calvet et al. investigated the effect of the environmental conditions on the bond behavior of different CFRP bars. The study indicated that at high temperatures the textured part of the CFRP bar separated from the bar (Calvet et al. 2015). CFRP had shown a better bond behavior than the reference steel bars did. The bond strength was 10% higher at the CFRP reinforcement system than at the steel (Calvet et al. 2015). Another study that investigated bond behavior was conducted by Altalmas et al. in 2015. The study analyzed the bond degradation of BFRP bars exposed to accelerated aging conditions. The bars were exposed to aggressive environment such as acid, saline, and alkaline. The results indicated that despite exposure, BFRP bars showed higher bond strengths to concrete than the ribbed GFRP did. The surface texture controlled the slippage resistance, as sand coated bars had better adhesion to concrete than ribbed bars regardless of the fiber type. GFRP bars exposed to acid solution suffered 25% loss in strength while the ones exposed to alkali and sea water lost 17% of its original strength (Altalmas et al. 2015).

Robert et al. investigated the behavior of GFRP reinforcing bars subjected to extreme temperatures. The study found that temperatures from 40° to 50 °C there was no significant effect on the tensile strength and modulus of elasticity (Robert 2010). Masmoudi et al. studied the effect of temperature ranging from 20 °C to 80 °C on the bond performance of GFRP bars in concrete. Eighty pull out specimens were tested to determine the bond behavior of the GFRP bars. The exposure period reached up to eight months and the highest temperature reached 80 °C. the study found that the exposure cause a 14% reduction in bond strength of the tested GFRP specimens (Masmoudi et al. 2011).

Research about the impact of exposure on BFRP bars using finite element analysis is limited. The main objective of this research is, therefore, to provide a FE model that can simulate the behavior of BFRP reinforced beams. The model would, then, provide much needed data about the flexural response of BFRP RC beams impacted by exposure. Over-reinforced beams would be used to examine the effect of varying BFRP bars modulus of elasticity on the flexural behavior of BFRP RC beams. Additionally, under-reinforced beams would be used to examine the effect of varying BFRP bars tensile strength on the flexural behavior of BFRP RC beams.

2 Brief Overview of the Experimental Program

The experimental program consisted of four RC beams reinforced with different configurations of BFRP bars that were exposed to UAE climate to investigate the effect of exposure to harsh environments on the capacity of the beams. The tested beams are 2200 mm long, 230 mm deep, and 180 mm wide with a clear span of 1900 mm as shown in Fig. 1. All beams were reinforced by ϕ8 stirrups spaced at 100 mm c/c to force flexural failure. The main flexural BFRP reinforcement are 2 ϕ 8, 2 ϕ 12, 2 ϕ 16 and 3 ϕ 12 for each beam, respectively. In addition, the tested specimens were reinforced with 2 ϕ 10 steel bars in the compression zone. Table 1 shows the tested beams designations and description. It should be noted that the beam specimens were loaded using two-point loading test at a displacement control mode rate of 1 mm/min.

The average concrete compressive strength (f'c) was found by averaging the values of crushing three cylinders. The average f'c of the beam specimens in this study is 36 MPa. In addition, uniaxial coupon tensile tests were conducted to measure the elastic modulus and tensile strength of BFRP and steel reinforcement. The average elastic modulus and tensile strength of BFRP bars was 59 GPa and 1200 MPa, respectively. In addition, the average Young's modulus and tensile strength of the steel bars was 200 GPa and 460 MPa, respectively.

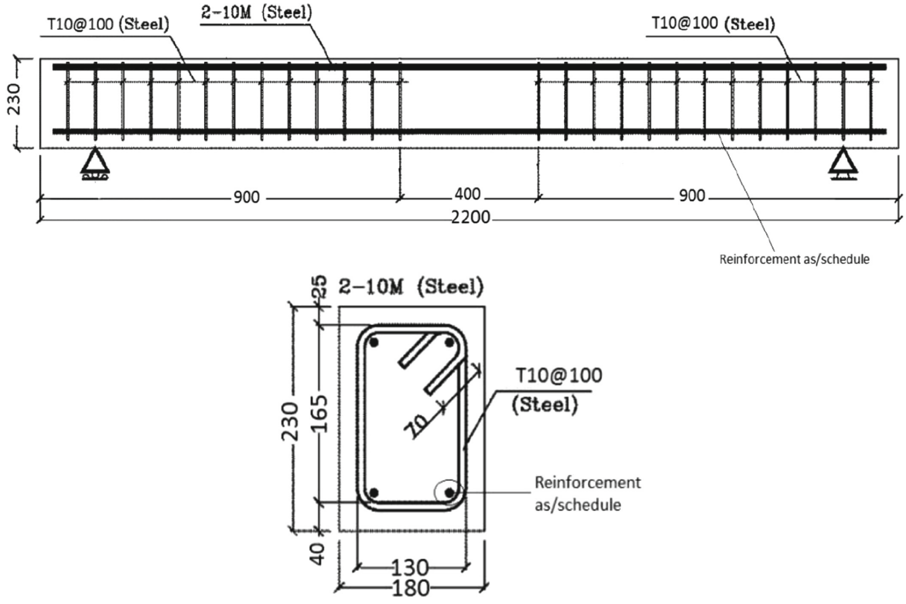

Fig. 1. Reinforcement details

Table 1. Test matrix

Beam designation	Description
2T8B	2 # 8 BFRP bars
2T12B	2 # 12 BFRP bars
3T12B	3 # 12 BFRP bars
2T16B	2 # 16 BFRP bars

2.1 Finite Element Modeling (FEM)

All beams investigated in this study were simulated using commercial finite element software (ABAQUS). The geometric and materials nonlinearities were captured by incorporating (*NLGEOM) parameter in the general static step. Full 3D beams were modeled and the load-displacement responses of four beams (2T8B, 2T12B, 3T12B, and 2T16B) were compared to the experimental results to validate the FE models. Following that, a parametric study was conducted to investigate the effect of reduction of modulus of elasticity of BFRP for over-reinforced beams (3T12B and 2T16B). In addition, the effects of reduction in tensile strength of BFRP for under-reinforced beams (2T6B) were investigated. Table 2 presents the modulus of elasticity and tensile strength of BFRP used to modeled beams in this study.

Table 2. FEM matrix

Beam designation	Modulus of elasticity (GPa)	Tensile strength (MPa)	Failure mode
Group 1 (3T12B; reduced modulus of elasticity)			
3T12B	53.1	1200	Concrete crushing
3T12B	47.2	1200	Concrete crushing
3T12B	41.3	1200	Concrete crushing
Group 2 (2T16B; reduced modulus of elasticity)			
2T16B	53.1	1200	Concrete crushing
2T16B	47.2	1200	Concrete crushing
2T16B	41.3	1200	Concrete v
Group 3 (FRP type)			
2T6B	59	1200	FRP rupture
2T6B	59	1080	FRP rupture
2T6B	59	960	FRP rupture
2T6B	59	840	FRP rupture

2.2 Material Properties

For the purpose of this study, three materials were defined in ABAQUS: concrete, steel and BFRP. The complex behavior of concrete was characterized by using concrete damage plasticity model provided by the software to simulate the nonlinearity of concrete material. Details of the parameters incorporated in concrete damage plasticity model are available in Abed et al. (2020). Compressive and tensile stress-strain curves that were input in the model were obtained based on the compressive strength of concrete as shown in Fig. 2.

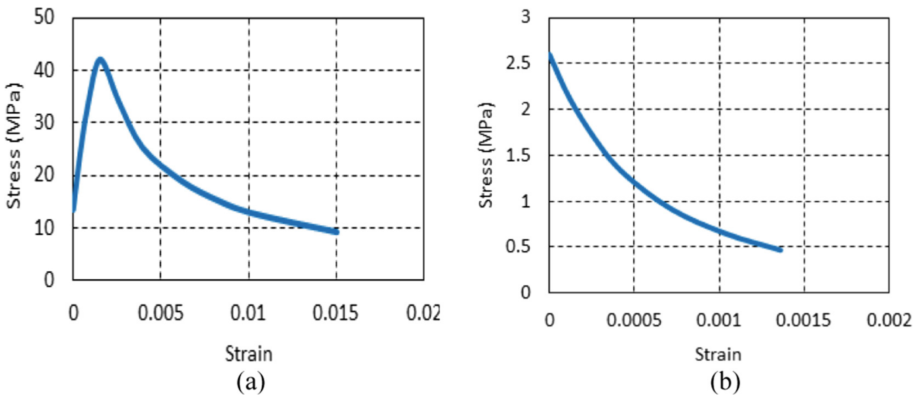

Fig. 2. Concrete material properties: (a) Compressive stress-strain curve; (b) Tensile stress-strain curve

Steel material, used in top reinforcement and stirrups, was defined to have an elastic modulus of 200 GPa and Poisson's ratio of 0.3. The plastic property, i.e. yield stress, was defined to be 460 MPa.

The behavior of BFRP bars is linear elastic, until it reaches its tensile capacity, after which it ruptures without yielding. All BFRP bars were modeled to have an elastic modulus of 59 GPa and Poisson's ratio 0.2. In over-reinforced beams the tensile capacity was defined to be 1200 MPa at zero plastic strain because failure is dominated by concrete crushing. On the other hand, the plastic property of under-reinforced beams was modeled to have a tensile strength of 1200 MPa at zero plastic strain.

2.3 Beam Geometry and Mesh Sensitivity

Steel and FRP bars were modeled as 2-node linear 3-D truss elements (T3D2) that are embedded in the concrete region. The concrete part was modeled as an 8-node linear 3D solid element with reduced integration (C3D8R). Mesh sensitivity was carried out to select the optimum mesh size that is not considered course and simulates the experimental results with minimum computational time. In this analysis, a mesh size of 30 mm was considered ideal for all beams. Figure 3 shows the reinforcement cage for a beam with 2 BFRP bars and mesh configuration for the beams modeled in this study. Four rigid plates were introduced to the model to apply onto the boundary conditions and reduce stress concentration on the beam in those areas. The interaction between the plates and the beam was modeled as surface-to-surface contact, with the beam being the slave surface and the plates as master surface. The boundary conditions at the bottom plates were a pin and a roller. In addition, a vertical displacement was applied at the top plates to mimic the applied load on the beam.

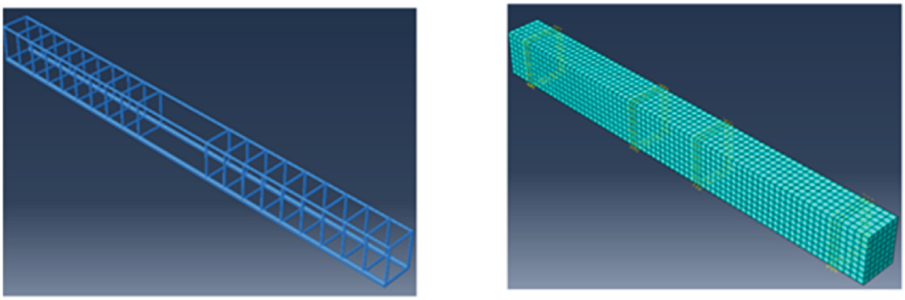

(a) (b)

Fig. 3. FEM model: (a) Reinforcement cage; (b) Mesh configuration

2.4 Model Verification

The validation of FE models was conducted by comparing load-midspan deflection responses of the experimental results and FE generated curves. Figure 4 shows the tested and simulated load-displacement curves for beams 2T8B, 2T12B, 2T16B, and 3T12B, respectively. It is can be seen from Fig. 4 that all simulated results are in good agreement with the experimental results at all stages of loading until failure. Mainly, the load at first crack, initial stiffness, and ultimate capacity of the beams maximum load and displacement of the FE models aligns with the experimental curves.

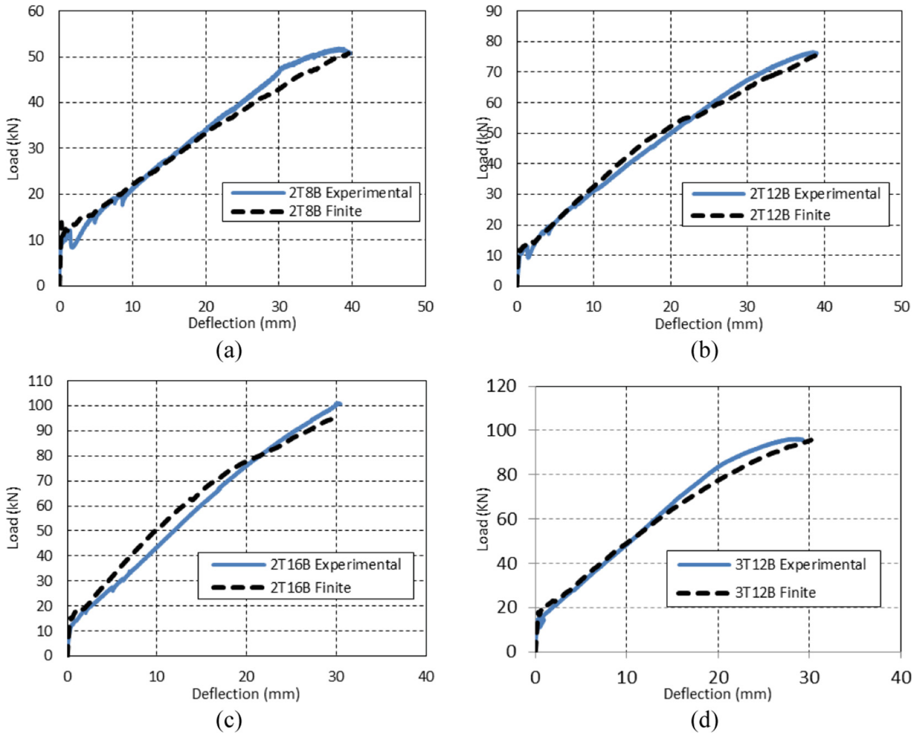

Fig. 4. Model verification for beams: (a) 2T8B; (b) 2T12B; (c) 2T16B; (d) 3T12B.

3 Discussion of Results

The verified models were utilized to carry out two parametric studies. Variations in the modulus of elasticity and tensile strength of BFRP were implemented and the flexural behavior of the varying models was observed.

Figure 5 presents the load versus midspan deflection behavior of the FE models examining the effect of reduction of the modulus of elasticity of BFRP on the flexural behavior of 3T12B beam. The modulus of elasticity values used were 1200 MPa, 1080 MPa, 960 MPa, and 840 or 0% 10%, 20%, and 30% reduction, respectively. The reduction of the modulus of elasticity caused a proportional reduction in the flexural capacity of the beam. The reduction becomes visible, only, after the first crack load which can be attributed to the similar concrete properties of the beam. Concrete properties control the behavior of the beam up until the first crack. After which, the properties of the BFRP controls the beams behavior.

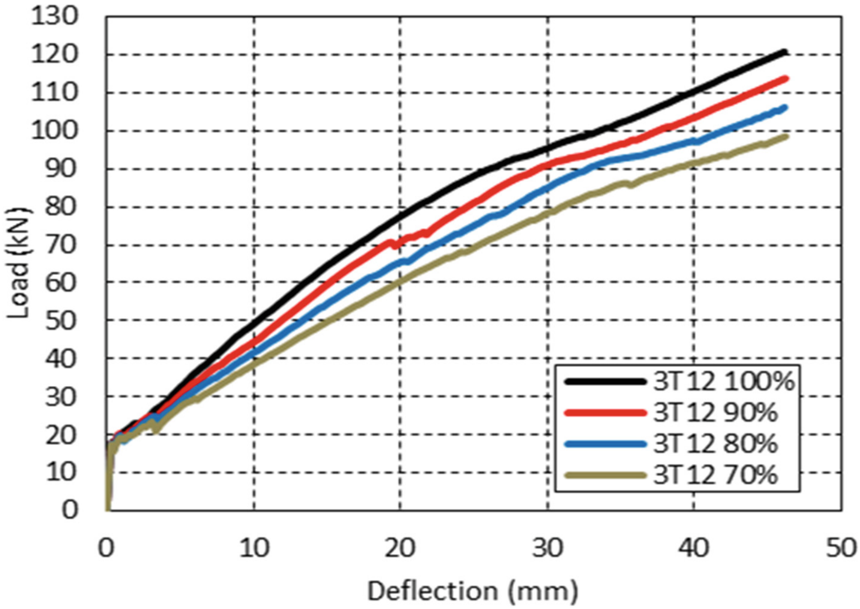

Fig. 5. Load-deflection curves for GROUP 1

Figure 6 presents the load versus midspan deflection behavior of the FE models examining the effect of reduction of the modulus of elasticity of BFRP on the flexural behavior of 2T16B beam. The modulus of elasticity values used the same values used in the 3T12B model. The reduction, also, showed a proportional reduction of the flexural capacity of the beam due to the decrease in the modulus of elasticity of the BFRP. Figure 5 and Fig. 6 show that beams with similar axial stiffness react to exposure in a similar fashion despite the detailing of the beam. The reduction in flexural capacity is not affected by the number of BFRP bars present in the tension zone.

Figure 7 presents the load versus midspan deflection behavior of the FE models examining the effect of reduction of the tensile strength of BFRP on the flexural behavior of 2T6B (under-reinforced) beam. The reduction in tensile strength caused a disproportional decrease in the flexural capacity of the beam. A reduction of 10% (as compared to the beam with 0% reduction), for example, impacted the capacity of the beam more than a reduction of 80% (as compared to the beam with 10% reduction.

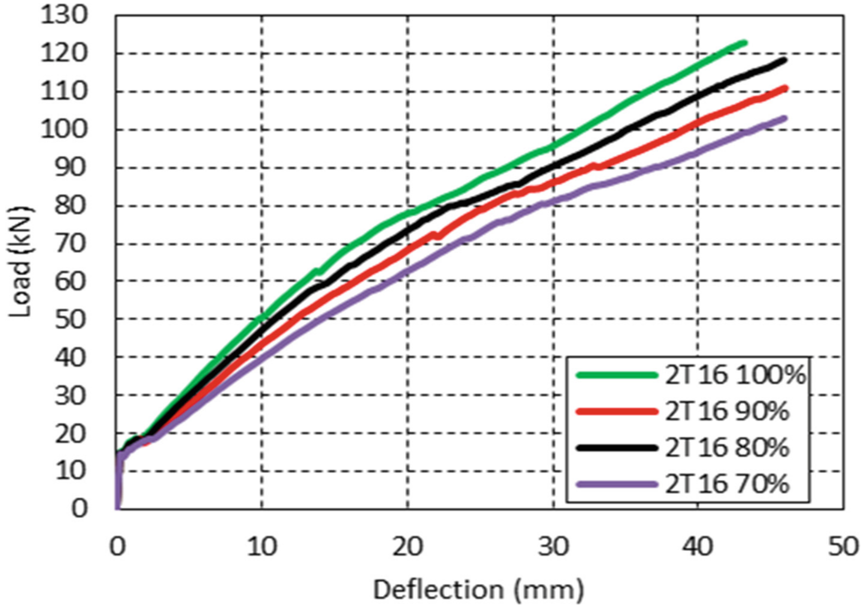

Fig. 6. Load-deflection curves for Group 2

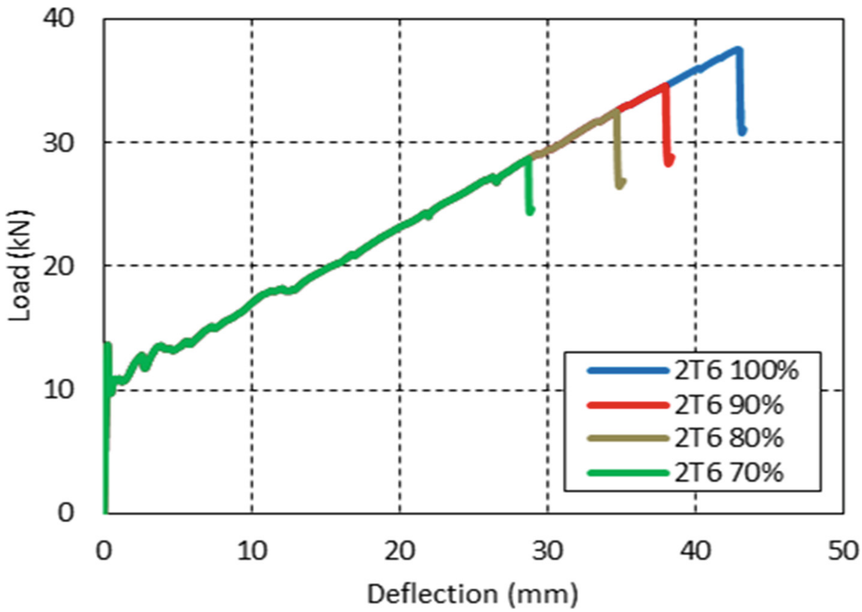

Fig. 7. Load-deflection curves for Group 3

4 Conclusions

After verifying the validity of the FE model using four BFRP RC beams, three nonlinear FE models were developed to study the response of RC beams reinforced in flexure with BFRP bars affected by exposure. Parametric analysis included variation in modulus of elasticity and tensile strength was performed. From the FE results, the following conclusions could be drawn. A decrease in the modulus of elasticity of BFRP bars (caused by exposure to harsh conditions) caused a proportional reduction in the flexural capacity of BFRP RC beams. The reduction in flexural capacity of the BFRP RC beams due to the reduction of the modulus of elasticity of the beams was not impacted by the detailing of the beam (i.e. number of reinforcement bars) of beams with similar axial stiffness. Reduction in the tensile strength of BFRP bars caused a disproportional decrease in the flexural capacity of BFRP RC beams.

References

ACI 440: Guide for the Design and Construction of Structural Concrete Reinforced with Fiber-Reinforced Polymer Bars. Farmington Hills, MI (2015)

Abed, F., Oucif, C., Awera, Y., Mhanna, H., Alkhraisha, H.: FE modeling of concrete beams and columns reinforced with FRP composites. Defense Technol. (2020, in press). https://doi.org/10.1016/j.dt.2020.02.015

Abed, F., El Refai, A., Abdalla, S.: Experimental and finite element investigation of the shear performance of BFRP-RC short beams. Structures **20**, 689–701 (2019). https://doi.org/10.1016/j.istruc.2019.06.019

Abed, F., Alhafiz, A.R.: Effect of basalt fibers on the flexural behavior of concrete beams reinforced with BFRP bars. Compos. Struct. **215**, 23–34 (2019). https://doi.org/10.1016/j.compstruct.2019.02.050

Abed, F., El-Chabib, H., AlHamaydeh, M.: Shear characteristics of GFRP-reinforced concrete deep beams without web reinforcement. J. Reinf. Plast. Compos. **31**, 1063–1073 (2012). https://doi.org/10.1177/0731684412450350

Al Rifai, M., El-Hassan, H., El-Maaddawy, T., Abed, F.: Durability of basalt FRP reinforcing bars in alkaline solution and moist concrete. Constr. Build. Mater. **243**, 118258 (2020). https://doi.org/10.1016/j.conbuildmat.2020.118258

Altalmas, A., El Refai, A., Abed, F.: Bond degradation of basalt fiber-reinforced polymer (BFRP) bars exposed to accelerated aging conditions. Constr. Build. Mater. **81**, 162–171 (2015). https://doi.org/10.1016/j.conbuildmat.2015.02.036

Al-Tamimi, A., Abed, F., Al-Rahmani, A.: Effects of harsh environmental exposures on the bond capacity between concrete and GFRP reinforcing bars. Adv. Concr. Constr. **2**(1), 1 (2014). https://doi.org/10.12989/acc.2014.2.1.001

Bedard, C.: Composite reinforcing bars: assessing their use in construction. Concr. Int. **14**, 55–59 (1992)

Calvet, V., Valcuende, M., Benlloch, J., Cánoves, J.: Influence of moderate temperatures on the bond between carbon fibre reinforced polymer bars (CFRP) and concrete. Constr. Build. Mater. **94** 589–604 (2015)

D'Antino, T., Pisani, M.A., Poggi, C.: Effect of the environment on the performance of GFRP reinforcing bars. Compos. B **141**, 123–136 (2018). https://doi.org/10.1016/j.compositesb.2017.12.037

El Messalami, N., El Refai, A., Abed, F.: Fiber-reinforced polymers bars for compression reinforcement: a promising alternative. Constr. Build. Mater. **209**, 725–737 (2019). https://doi.org/10.1016/j.conbuildmat.2019.03.105

El Refai, A., Abed, F.: Concrete contribution to shear strength of beams reinforced with basalt fiber-reinforced bars. J. Compos. Constr. **20** (2016).https://doi.org/10.1061/(asce)cc.1943-5614.0000648

El Refai, A., Abed, F., Altalmas, A.: Bond durability of basalt fiber–reinforced polymer bars embedded in concrete under direct pullout conditions. J. Compos. Constr. **19**(5), 04014078 (2014). https://doi.org/10.1061/(ASCE)CC.1943-5614.0000544

El Refai, A., Abed, F., Al-Rahmani, A.: Structural performance and serviceability of concrete beams reinforced with hybrid (GFRP and steel) bars. Constr. Build. Mater. **96**, 518–529 (2015). https://doi.org/10.1016/j.conbuildmat.2015.08.063

Elgabbas, F., Benmokrane, B., Ahmed, E.: Flexural behavior of concrete beams reinforced with ribbed basalt-FRP bars under static loads. J. Compos. Constr. **21** (2017). https://doi.org/10.1061/(asce)cc.1943-5614.0000752

Fam, A., Tomlinson, D.: Performance of concrete beams reinforced with basalt FRP for flexure and shear. J. Compos. Constr. **19** (2015). https://doi.org/10.1061/(asce)cc.1943-5614.0000491

Hollaway, L.C.: The evolution of and the way forward for advanced polymer composites in the civil infrastructure. Constr. Build. Mater. **17**, 365–378 (2003). https://doi.org/10.1016/S0950-0618(03)00038-2

Masmoudi, R., Masmoudi, A., Ouezdou, M.B., Daoud, A.: Long-term bond performance of GFRP bars in concrete under temperature ranging from 20 °C to 80 °C. Constr. Build. Mater. **25**, 486–493 (2011)

Robert, M.: Behavior of GFRP reinforcing bars subjected to extreme temperatures. J. Compos. Constr. **14**, 353–360 (2010). https://doi.org/10.1061/(ASCE)CC.1943-5614.0000092

Robert, M., Cousin, P., Benmokrane, B., Canadian Society for Civil Engineering Annual Conference St. Johns NC: Behaviour of GFRP reinforcing bars subjected to extreme temperatures. In: Proceedings, Annual Conference - Canadian Society for Civil Engineering, vol. 3, pp. 1587–1596

Sim, J., Park, C., Moon, D.Y.: Characteristics of basalt fiber as a strengthening material for concrete structures. Compos. B **36**, 504–512 (2005). https://doi.org/10.1016/j.compositesb.2005.02.002

SIMULAI: Abaqus/CAE User's Manual, Rising Sun Mills, RI (2019)

Wang, M., Zhang, Z., Li, Y., Li, M., Sun, Z.: Chemical durability and mechanical properties of alkali-proof basalt fiber and its reinforced epoxy composites. J. Reinf. Plast. Compos. **27**, 393–407 (2008)

Wu, G., Dong, Z.-Q., Wang, X., Zhu, Y., Wu, Z.-S.: Prediction of Long-Term Performance and Durability of BFRP Bars under the combined effect of sustained load and corrosive solutions. J. Compos. Constr. **19**, 04014058 (2015) . https://doi.org/10.1061/(ASCE)CC.1943-5614.0000517

Yan, F., Lin, Z.: Bond durability assessment and long-term degradation prediction for GFRP bars to fiber-reinforced concrete under saline solutions. Compos. Struct. **161**, 393–406 (2017). https://doi.org/10.1016/j.compstruct.2016.11.055

Manufacturing and Mechanical Testing of Casuarina Glauca Blockboards

Nour Abdellatif[1], Mohamed Darwish[2](✉), Khaled Nassar[1], Passant Youssef[1], Abdallah Dardir[1], Abdulrahman Ahmed[1], Mahmoud Eltamimy[1], Mohamed Mamdouh[1], and Rami Abdelazim[1]

[1] Department of Construction Engineering, American University in Cairo, Cairo, Egypt
[2] Department of Construction and Building Engineering, Alahram Canadian University, American University in Cairo, Cairo, Egypt
mdarwish@aucegypt.edu

Abstract. Wood, or timber, is light, cheap, and easy to transport and work with. On the contrary, reinforced concrete is more expensive, heavy & difficult to transport and slower to build. Previous research has proven that relatively cheap Casuarina Glauca wood could have sufficiently high strength that makes it a strong candidate for structural usage. In the construction field in Egypt, most of the used wood is blockboard composed from imported wood. The importing of wood represents a significant segment and Egypt invests a lot of its money in this segment, thus a research such as this one would significantly help Egypt to save money in the import business. This research aims to produce and test Egyptian blockboard made from Casuarina Glauca wood farmed in Egypt. The blockboards were produced and tested for their mechanical properties and compared to their imported counterparts. Moreover, these blockboards proved to be of a sufficiently high strength. Based on the results, this engineered wood product could be a structurally sound alternative for structural usage.

1 Introduction

Based on the research done, the Egyptian construction market consumption of wood is draining the Egyptian market from a lot of investment and is considered costly since most of the wood products in Egypt is imported. Egypt started importing wood since 1957 and right now the total imports of wood costs approximately $1.57 billion USD. Which is about 2% of the total exports in Egypt. Using such mass of money in investing in the Egyptian market and enhancing the wood industry in Egypt which currently have high quality resources as seen in country report. Egypt is trying to advance in the forestation sector, thus giving manufacturers the ability to use such products from the Egyptian Agriculture. Egypt is planting 3 tropical trees in Upper Egypt named Khaya, Teak and Neem. Also some water treatment plants in Egypt grows Casuarina trees near wastewater since such trees can endure and survive using wastewater. This shows how the forestation in Egypt is in a phase of expansion. Nowadays, The Seed Bank that is developed in the past years in Egypt carries tests and experiments new techniques in breeding trees in Egypt and also stores seeds and plants coming abroad from other countries. This ensures

H. Shehata and S. El-Badawy (Eds.): *Sustainable Issues in Infrastructure Engineering*, SUCI, pp. 14–22, 2021.
https://doi.org/10.1007/978-3-030-62586-3_2

the continuity of the improvement in the Egyptian wood forestation. Nowadays, Egypt is in a shortage of producing wood (FAS 2015).

Meanwhile a previous study by Hussein et al. (2019a) have covered the mechanical properties of different types of Casuarina. Within that study, the Glauca specie of Casurina was proven to be even stronger than several types of oaks. The study was further extended to study the different properties of that wood within different percentages of moisture content Hussein et al. (2019b).

The high strength of that type of wood encouraged Mahmoud et al. (2019) to further study its mechanical properties, its grading categorization and the usage of coatings to protect it. Furthermore, Mahmoud et al. (2019b) have studied its usage to design a 12-m span truss and have experimentally proven that the truss members made of Casuarina Glauca could carry even more than the design loads.

Several researchers like Zanuttini and Cremonini (2002) and Haseli et al. (2018) have studied the manufacturing of blockboards but unfortunately none of them have manufactured blockboards of sufficient strength using cost-effective raw materials like Casuarina Glauca. Furthermore, other researchers like Youssef et al. (2019) have used Egyptian wood waste to produce an engineered wood product but again it was not as strong as the parent wood itself.

The current research focuses on using the locally available and relatively strong Casuarina Glauca wood in manufacturing blockboards. Consequently, the Egyptian blockboard produced in this research could fill a lot of the gaps as it uses the locally available, cost-effective and strong Casuarina Glauca wood to produce a structurally sound and cost-effective blockboard. This was done through manufacturing several thicknesses of the blockboard, testing them till failure and comparing their results with the market-available imported counterparts. Furthermore, a cost comparison between the locally manufactured and imported blockboards was performed. The Egyptian blockboard proved to be more sound in terms of strength and cost-effectiveness and would be a promising candidate to be used in building structures as to be seen in this paper.

2 Manufacturing and Testing Procedures

2.1 Production of Casuarina Glauca BlockBoard

The process of blockboard production could be summarized into eight main steps which are:

1. Obtaining the Casuarina Glauca wood from the supplier and obtaining the veneer wood.
2. Preparation of the wood, profiling the wood so that it has a smooth surface.
3. Sawing the wood into blocks or battens with a dimension of (35 * 18 * 400 mm) with a clean saw and this is crucial for two reasons the first is that when the battens are arranged next to each other no voids would be present between them that would weaken the blockboard and the second is for a better cohesion between the battens.
4. Arranging the wood in a brick-like pattern so that we don't have any weak planes inside of the board by not having two joints next to each other as shown in Fig. 1.

Fig. 1. The arrangement of wood within a blockboard panel.

Fig. 2. The sandwiching of wood in between the two veneer layers.

5. Formulating the glue, the glue that was used was a glue consisting of a risen and a hardener. The risen was Phenol formaldehyde and the hardener was ammonia.
6. Equally spreading the glue on the veneer and checking not to miss a space.
7. Taking the blocks or battens with the arrangement done in step 4 and placing them on the veneer and placing the other layer of the glued veneer, with this step we have a sandwich like structure with a veneer on top and bottom as shown in Fig. 2.
8. Applying heat and pressure on the block board so that the glue wood hardens and gain a higher strength and no voids exists between the battens and the veneer. The heat and pressure was applied for 12 min using the hot-press device and then the board would be removed.

2.2 Testing of Casuarina Glauca Blockboard

In construction, wood in most likely used as a compression member or a member to resist bending, it is not likely to see wood used as a member to carry a tension force or torsion, thus when testing the blockboard compression and the 4-point bending tests were performed. Compression testing was performed twice; parallel to the wood grain and perpendicular to the wood grain. Two different orientations for the 4-point bending were tested; one orientation was the load being applied to the thickness dimension thus the resisting section was the thickness of the blockboard and the other orientation was the specimen width was the resisting section. The sizing of the specimens for the bending samples the specimens size was 18 mm * 92.5 mm * 400 mm which allowed a clear span of 310 mm and for the compression samples the specimens size was 18 mm * 92.5 mm * 133 mm. In the compression tests the specimens of the blockboard had a dimensioning of 18 mm * 100 mm * 130 mm where the 130 mm is the height and the 100 mm is the width and the 18 mm is the thickness. The load was applied on the 100 mm * 18 mm surface when the compression test was parallel to the grain as shown in Fig. 3a. Meanwhile, the load was applied on the 130 mm * 18 mm surface when the compression test was perpendicular to the grain as shown in Fig. 3b. The specimen was done in these dimensions to avoid buckling thus testing for compressive strength of the wood. The testing of these specimens was done on a MTS machine and according to the ASTM and the referred ASTM tests were D143-14, D4761-19 with some deviations from the ASTM. In the compression and bending tests, the specimen tested was placed in the MTS and a metal disc was placed on the sample as to insure that the load would be well distributed along the specimen. In the perpendicular compression test the load was applied at a rate of 2 mm/min while in the parallel compression test the rate was 4 mm/min the reason for increasing the rate was due to knowing that the wood is anisotropic material and can carry more loads in the direction of parallel to the fiber. In the 4-point bending test the rate was kept constant 2 mm/min regardless of the orientation.

a. Testing for compression parallel to the grains

b. Testing for compression perpendicular to the grains

Fig. 3. The experimental set-up for the compression tests.